

Structure and permeation of organic–inorganic hybrid membranes composed of poly(vinyl alcohol) and polysilisesquioxane†

Qiu Gen Zhang, Qing Lin Liu,* Feng Feng Shi and Ying Xiong

Received 14th April 2008, Accepted 16th July 2008

First published as an Advance Article on the web 26th August 2008

DOI: 10.1039/b806303f

Organic–inorganic hybrid membranes with high separation performance were prepared by the incorporation of polysilisesquioxane (PSS) into a poly(vinyl alcohol) (PVA) matrix in order to solve the trade-off relationship between the selectivity and permeability of PVA membranes. The incorporation of the PSS resulted in a change in the physical and chemical structure of the hybrid membranes. The crystalline region in the hybrid membranes decreased with increasing PSS content. The hydrophilicity of the hybrid membranes increased when the PSS content is below 3 wt%, and then decreased. Silica particles formed on the surface and in the interior of the hybrid membranes due to the PSS conglomeration, and the surface roughness of the hybrid membranes increased linearly with increasing PSS content. The trade-off between permeability and selectivity was successfully solved using the hybrid membranes in pervaporation dehydration of tetrahydrofuran. The permselectivity and flux of the hybrid membranes increased simultaneously when the PSS content was below 2 wt%, whereas the permselectivity decreased when the PSS content was above 2 wt%. The hybrid membrane containing 2 wt% PSS had the highest separation factor of 1810.

Introduction

Pervaporation has been widely studied as means of separation of liquid solutions, particularly for the separation of azeotropic or close-boiling-point mixtures^{1,2} due to its simplicity and energy-saving efficiency compared with conventional distillation processes. Membranes are the key factor in pervaporation separation processes, most of which are polymers owing to their cheap and film-forming ability. However, polymeric membranes have the inherent drawback of the trade-off between permselectivity and permeability. This means that membranes which are more permeable are generally less selective and *vice versa*.^{3–6} Thus, how to solve the trade-off inherent in polymeric membranes and prepare membranes having high separation performance is an important and interesting task.

Organic–inorganic hybrid materials not only combine the important properties from both organic and inorganic worlds but also create entirely new compositions with unique properties, which offer specific advantages for the preparation of artificial membranes exhibiting high selectivity and flux, as well as good thermal and chemical resistances. The hybridization of organic and inorganic components seems to be a facile and feasible way to solve the trade-off involved in polymeric membranes.^{7–10} Organic–inorganic hybrid membranes can be classified into two categories according to the interaction between organic and inorganic components.^{9–11} “Type I” hybrid membranes are commonly prepared by simply blending polymer and inorganic filler, where the

organic and inorganic components interact through weak hydrogen bonding, Van der Waals or electrostatic forces. “Type II” hybrid membranes are generally synthesized by sol–gel reaction between polymer (or monomer) and inorganic precursor (or oligomer), where the organic and inorganic components are linked by a strong covalent bond, resulting in a homogeneous hybrid material at the molecular level. There are many adjustable parameters (monomer type and concentration, synthesis condition, *etc.*) that can be varied to obtain Type II hybrid membranes with high performance and functionality. These involve various areas of chemistry (organic, inorganic, organometallic and polymer), and thus researchers currently pay more attention to this field. Many Type II hybrid membranes are used in fuel cells,^{12–14} gas separation,^{8,10,15} or as switchable molecular filters,¹⁶ *etc.* In pervaporation processes, this type of hybrid membrane has been widely studied; they include chitosan, quaternized chitosan, poly(butylmetacrylate-*co*-vinyltriethoxysilane), polyurethane, poly(vinyl alcohol-*co*-acrylic acid), and poly(vinyl alcohol) silica-based hybrid membranes.^{17–25} Such hybrid membranes have higher separation efficiencies than their original counterparts.

Poly(vinyl alcohol) (PVA) is one of the most important materials for pervaporation dehydration of organic mixtures due to its good chemical stability, film-forming ability and high hydrophilicity.^{1,25} However, there are two drawbacks, namely the trade-off between permeability and selectivity and the swelling of PVA membranes in aqueous solution.²⁶ To control membrane swelling and improve selectivity, some methods have been attempted, such as cross-linking, filling, blending, and grafting.^{27–30} Urugami²³ and Kariduraganavar^{31,32} prepared PVA–tetraethoxysilane hybrid membranes through a sol–gel reaction for the dehydration of ethanol, isopropanol and acetic acid. The hybrid membranes reported have a lower degree of swelling in aqueous solutions and higher water permselectivity

Department of Chemical and Biochemical Engineering, College of Chemistry and Chemical Engineering, Xiamen University, Xiamen, 361005, China. E-mail: qlliu@xmu.edu.cn

† Electronic supplementary information (ESI) available: Preparation of the samples for XRD, SEM and TEM; Fig. S1 and S2. See DOI: 10.1039/b806303f

than pristine PVA membranes. In previous studies,^{25,26,33,34} we prepared PVA- γ -aminopropyltriethoxysilane (APTEOS) hybrid membranes through a sol-gel reaction between PVA and APTEOS for the dehydration of alcohol. The trade-off between permeability and selectivity was successfully solved using those hybrid membranes. Water flux and permselectivity increased simultaneously.

In this paper, low molecular weight polysilisesquioxane (PSS) was synthesized from APTEOS *via* a sol-gel reaction. The PSS was inserted into the PVA matrix resulting in the formation of PVA-PSS organic-inorganic hybrid membranes for pervaporation dehydration of tetrahydrofuran (THF). PSS has high hydrophilicity due to its amino and silanol groups, which can make the hybrid membranes increase or retain preferential sorption for water. On the other hand, the PSS dispersed in the PVA matrix will prevent crystalline regions from forming in the matrix and modify the microstructure of the hybrid membranes, which will favor penetrant diffusion through the membranes. Thus the trade-off between permeability and selectivity will be solved using the PVA-PSS hybrid membranes.

Experimental section

Materials

PVA with a polymerization degree of 1750 ± 50 and a hydrolysis degree of 98%, was supplied by Sinophatm Chemical Reagent Co. Ltd (China). APTEOS was purchased from Shanghai Yaohua Chemical Plant (China). All other solvents and reagents of analytical grade, were purchased from Sinophatm Chemical Reagent Co. Ltd, and used without further purification.

Synthesis of polysilisesquioxane

Polysilisesquioxane (PSS) was synthesized from APTEOS by a sol-gel reaction. The APTEOS was polymerized in a three-necked flask with methanol as a solvent with stirring at 60 °C for 24 hours. The APTEOS content was 15 mol % in the reaction solution, and the molar ratio of water to APTEOS was 1.5 under stoichiometric conditions for complete hydrolysis. The temperature was controlled by a thermostat water bath with an accuracy of ± 1 °C. Hydrochloric acid was used as catalyst with the pH adjusted to 5. After the reaction was complete, the solvent was removed in vacuum at 60 °C, and the resulting solid was washed three times with cyclohexane. The washed solid was then completely dried in a vacuum oven at 80 °C, and a white solid was finally obtained.

Preparation of hybrid membranes

PVA was dissolved in deionized water at 90 °C for 3 hours to obtain a homogeneous solution. The hot PVA solution was filtered, a measured amount of PSS was then added, and the mixture was stirred at 60 °C for 1 hour and subsequently dispersed by ultrasound for 1 hour. The resulting homogeneous solution was cast onto a clean glass plate with the aid of a casting knife. The membranes were allowed to dry at 40 °C for 10 hours. The dried membranes were subsequently peeled off and the solvent allowed to evaporate completely in vacuum at 80 °C for another 10 hours. The obtained membranes were transparent,

with a thickness of 20 ± 1 μm , although the transparency of the hybrid membranes decreased slightly with increasing PSS content. The total mass fraction of the PVA and PSS in the homogeneous solution was 4 wt%, and the weight percentage of PSS to PVA plus PSS was set at 0, 1, 2, 3, 4, 5, 6, 8 and 10 wt%. The resulting hybrid membranes were designated as HM-*X*, where *X* indicates the weight percentage of the PSS in the membranes.

Characterization

The chemical structure of the PSS and hybrid membranes were characterized using a Nicolet infrared spectrometer (FTIR 740SX, USA) equipped with attenuated total reflectance (ATR) accessories, and by solid-state NMR spectroscopy. The FTIR spectrum of the PSS was obtained by transmission, and the membranes were investigated by ATR. The solid-state ²⁹Si NMR spectra were measured at 25 °C using an AVANCE AV 400 MHz spectrometer (Bruker Co., Switzerland) with 4 mm CP/MAS (cross polarization/magic angle spinning) probe with a spinning rate of 6000 circuits s⁻¹ and a resonance frequency of 79.49 MHz. Cross-polarization was used in the NMR measurements with a contact time of 5 ms and a repeated delay time of 3 s. The solid powder samples were obtained by scraping the membrane surface with knife. These samples were dried in vacuum at 30 °C for 24 hours before testing. The ²⁹Si spectra recorded were edited by NMR soft MestRe-C V. 3.0.

The physical structure of the membranes was studied at 25 °C by X-ray powder diffraction (XRD, Panalytical X'pert, Enraf-Nonious Co. Holland) using Cu K α radiation with a step size of 0.0167° and a scan speed of 0.167° s⁻¹ in the range 5 to 45°. The morphology and microstructure of the membranes were measured using scanning electron microscopy (SEM, XL30ESEM, Philips), and high-resolution transmission electron microscopy (HRTEM, TECNAI F-30, Philips). The topography of the membrane surfaces was determined by atomic force microscopy (AFM) (Nanoscope IIIa multimode SPM, Digital Instruments, USA) with a commercial Si probe in the tapping mode at 25 °C. After image acquisition, the root-mean-square (RMS) roughness, R_q , was obtained by a program in the AFM image processing toolbox. The sample preparation for XRD, SEM and TEM is detailed in Part A of ESI†.

The static water contact angles on the surface of the membranes were measured at 25 °C and a relative humidity of 46% by a contact angle meter (SL200B, Shanghai Solon Tech Inc. Ltd.), and the density of the membranes was measured by a flotation method using cyclohexane at 25 °C.

Pervaporation

Pervaporation experiments were carried out on a PERVAP 2201 instrument (Sulzer Chertiest, Germany) at 50 °C with the pressure on the permeate side kept at 10 mbar and the feed flow rate at 90 L h⁻¹. The effective membrane area was 71 cm². Aqueous THF solution (90 wt%) was used as the feed. The permeate was collected in liquid nitrogen cold-traps and measured by gas chromatography to determine the concentration.

The permeation properties of the membranes were characterized by a total permeation flux (J) and separation factor (α), which can be calculated from the following equations.

$$J = W/At \quad (1)$$

$$\alpha = (P_{\text{water}}/P_{\text{THF}})/(F_{\text{water}}/F_{\text{THF}}) \quad (2)$$

where W is the mass of the permeate (kg), A is the area of the membrane in contact with the feed mixture (m^2), t is the permeation time (h), P_{water} and P_{THF} are the mass fractions of water and THF in the permeate respectively, and F_{water} and F_{THF} are the mass fractions of water and THF in the feed mixture respectively.

Results and discussion

Synthesis of polysilisesquioxane

Polysilisesquioxane (PSS) is a silica-based organic-inorganic hybrid material, which is generally prepared by hydrolysis/condensation of RSiX_3 ($X = \text{Cl, OR, H}$) under acid or base catalysis.¹¹ Firstly, APTEOS was hydrolyzed in the presence of acid catalyst (HCl) to form silanol. Then the low molecular weight PSS was produced as a white powder *via* the condensation between the resulting silanol (see Fig. 1). The obtained white powder is very soluble in water, methanol and ethanol, with a molecular weight of about 1000–2000 g mol^{-1} measured by Fourier transform ion cyclotron resonance mass spectrometry (APEX II, Bruker Daltonik, Bremen, Germany).

The chemical structure of the PSS was analyzed by solid-state ^{29}Si NMR and FTIR spectra, as shown in Fig. 2(a) and Fig. 3(a) respectively. The terminal structural units of siloxane precursor, which have three functional groups responsible for condensation reactions, give rise to three signals, T_1 , T_2 and T_3 . The T_1 units contain two residual hydroxyl groups, the T_2 units contain one residual hydroxyl group, and the T_3 units indicate that all the three hydroxyl groups take part in the reaction.³⁵ There are three peaks at chemical shifts of 45.94, 54.72 and 62.92 in the solid-state ^{29}Si NMR spectrum of the PSS (Fig. 2(a)), which correspond to the T_1 , T_2 and T_3 units respectively.³⁶ This suggests that PSS has all three structural units, and the hydroxyl groups in the T_1 and T_2 units are available to react with the PVA chains in

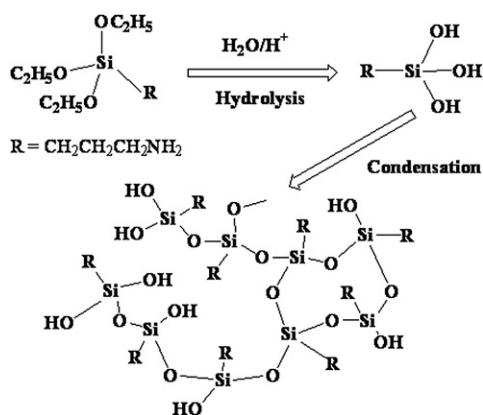


Fig. 1 Reaction scheme for the synthesis of PSS.

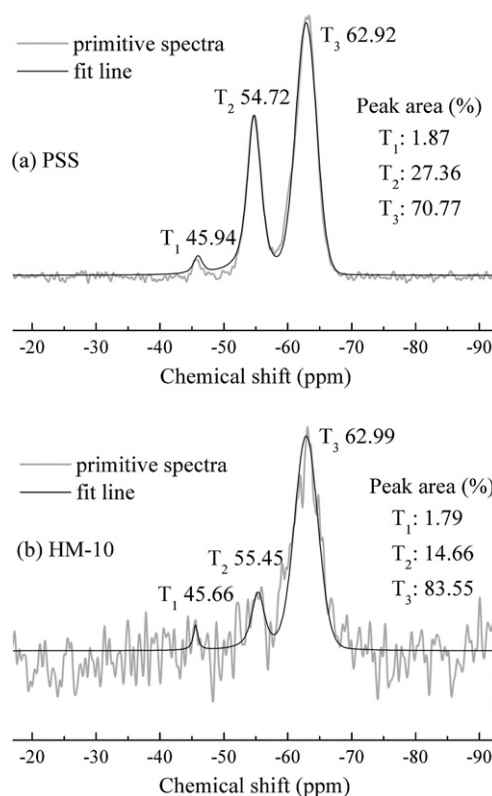


Fig. 2 Solid-state ^{29}Si CP MAS-NMR spectra of (a) PSS, (b) HM-10.

preparing the hybrid membranes. Fig. 3(a) shows the FTIR spectrum of the PSS at $3850\text{--}700\text{ cm}^{-1}$, and the characteristic peaks were assigned in the spectrum. In particular, the peaks at 1130 and 1030 cm^{-1} are associated with the stretching of Si-O-Si groups, and the peak at 917 cm^{-1} is due to the Si-OH groups. This confirms the existence of Si-OH and that the condensation reaction between silanols has taken place.

Formation of hybrid membranes

In preparing the hybrid membranes, PSS was dispersed homogeneously in the PVA solution by stirring and ultrasound. During the membrane drying process, the dehydration between the hydroxyl groups in the PSS and the hydroxyl groups in the PVA formed siloxane bonds which are the crosslink spots in the hybrid membranes (Scheme 1). On the other hand, the PSS will absorb due to the condensation of silanol with the PSS, resulting in the formation of the inorganic phase domain in the PVA matrix (Scheme 2).

Fig. 2(b) shows the solid-state ^{29}Si NMR spectrum of HM-10. Three peaks were also observed, the peak intensity of the T_2 units being weaker than for PSS, and the peak intensity of the T_3 units being stronger than for PSS. The T_1 , T_2 and T_3 peak area percentages are shown in Fig. 2. There are fewer T_1 units in HM-10 than in PSS. This suggests that some of the T_1 units changed into T_2 or T_3 units. This may be because the T_1 units are located mainly in the interior of the PSS. In the HM-10, the number of T_2 units decreased significantly, and the number of T_3 units underwent an observable increase. This suggests that a large number of the T_2 units in the PSS took part in

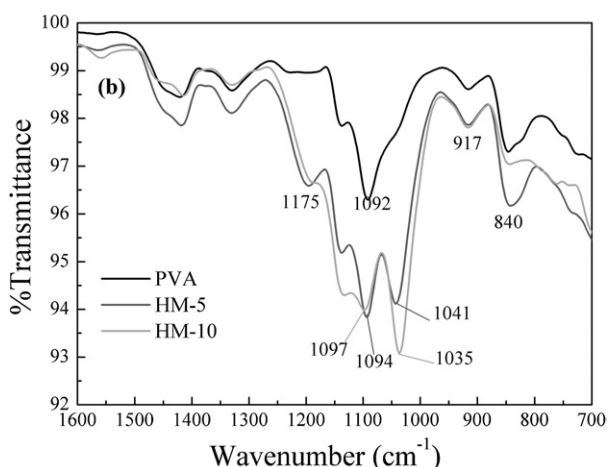
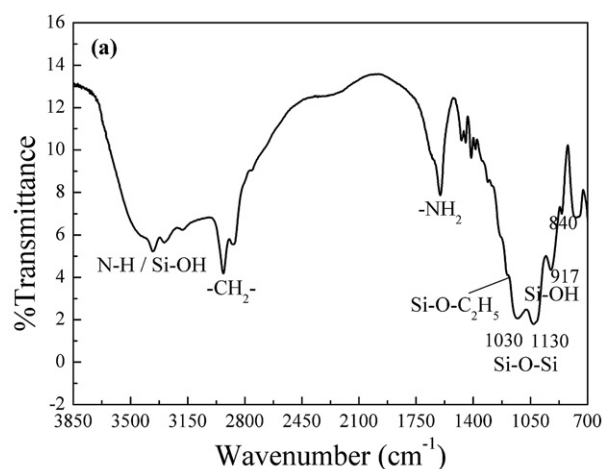
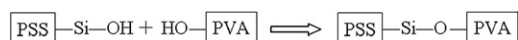
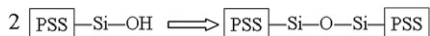


Fig. 3 FTIR spectra of (a) PSS, (b) PVA and hybrid membranes.



Scheme 1 Dehydration reaction between PSS and PVA.



Scheme 2 Condensation reaction for PSS.

condensation reaction, resulting in a change into the T_3 units in the hybrid membranes. Fig. 3(b) shows the FTIR spectra of the PVA and hybrid membranes at 1600–700 cm^{-1} . With increasing PSS content, the 917 cm^{-1} peak (Si–OH and C–OH) enhanced, a 1045 cm^{-1} peak arose due to the formation of Si–O–C groups, and the 1090 cm^{-1} peak shifted to the left owing to the existence of Si–O–Si groups (1130 cm^{-1}). As noted previously, the Type II hybrid membranes composed of PVA and PSS were prepared successfully, as confirmed by solid-state ^{29}Si NMR and FTIR spectra.

The physical structure of the membranes was investigated by XRD, as displayed in Fig. 4. The characteristic peak of the PVA and hybrid membranes appeared at $2\theta \approx 20^\circ$, and the peak intensity decreased continuously from PVA to HM-10. This suggests that the crystalline region of the hybrid membranes

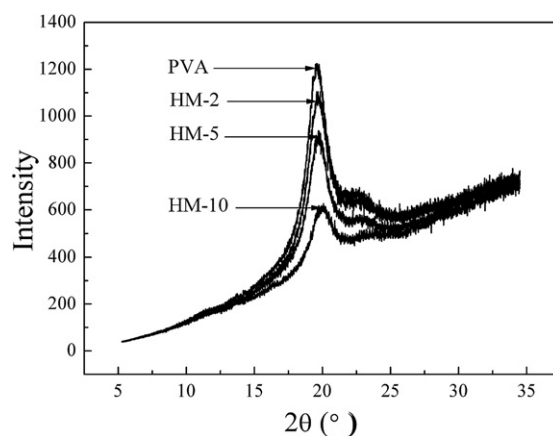


Fig. 4 XRD patterns of the PVA and hybrid membranes.

decreased with increasing PSS content. This is because the PSS dispersed in the PVA matrix disordered the arrangement of the PVA chains and hence prevented the formation of the crystalline region in the PVA matrix. According to the solution–diffusion mechanism, the amorphous region increased, which favors the diffusion of components and results in an increase of permeation flux.²⁶

The hydrophilicity of the PVA and hybrid membranes was studied by measuring the static water contact angles, as shown in Fig. 5. The hydrophilicity of the surface of the hybrid membranes at first increases with increasing PSS content, and then decreases when the PSS content is above 3.0 wt%. This is because introducing PSS into the PVA matrix disorders the PVA chains and decreases the PVA crystallinity. All these result in an increase of the dissociative hydroxyl groups on the PVA chains, and hence lead to an increase in the hydrophilicity of the hybrid membranes. However, the number of hydroxyl groups decrease significantly because of fast condensation between the hydroxyl groups with PSS when the PSS content is above 3 wt%, resulting in a decrease of the hydrophilicity of the hybrid membranes. With increasing PSS content, the density of the hybrid membranes increases because of cross-linking between the PSS and PVA, making the amorphous region more compact (Fig. 5).

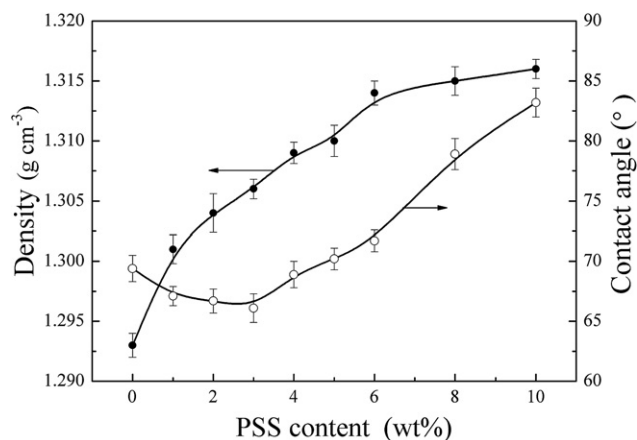


Fig. 5 The static water contact angles and the density of the PVA and hybrid membranes at 25 °C.

Structure of hybrid membranes

The topography of the membrane surfaces was determined by AFM. Fig. 6 shows the AFM images of the surface of the PVA and hybrid membranes. With increasing PSS content, the roughness of the hybrid membrane surface (R_q) increased linearly from 1.799 nm to 98.295 nm (see Fig. S1†). Ridges and valleys are observed on the surface of the hybrid membranes, which become bigger with increasing PSS content. This is because the PSS dispersed on the surface of the hybrid membranes could undergo condensation polymerization to form silica particles, resulting in an increase in the roughness. Furthermore, the PSS could disorder the PVA chains, resulting in a stress change in the PVA matrix which leads to surface deformation of the hybrid membrane. These rough surfaces will be in contact with the feed during pervaporation processes, which favors the feed diffusion. The surface

morphology of the hybrid membranes was also investigated by SEM. An inorganic phase is observed on the surface of the hybrid membranes, and the surface becomes rougher with increasing PSS content (see Fig. S2†).

Fig. 7 shows the cross-sectional micrographs of the hybrid membranes with different PSS content. When the PSS content is below 2 wt%, the PSS disperses homogeneously in the hybrid membranes and silica particles do not form. Silica particles are observed in the cross-sectional image of the hybrid membrane containing 3 wt% PSS content (HM-3), which disperse homogeneously in the membrane matrix and grow bigger with increasing PSS content. When the PSS content is above 9 wt%, a large amount of PSS congregates due to the PSS condensation, resulting in the formation of a large inorganic phase domain and a coarser hybrid membrane interior.

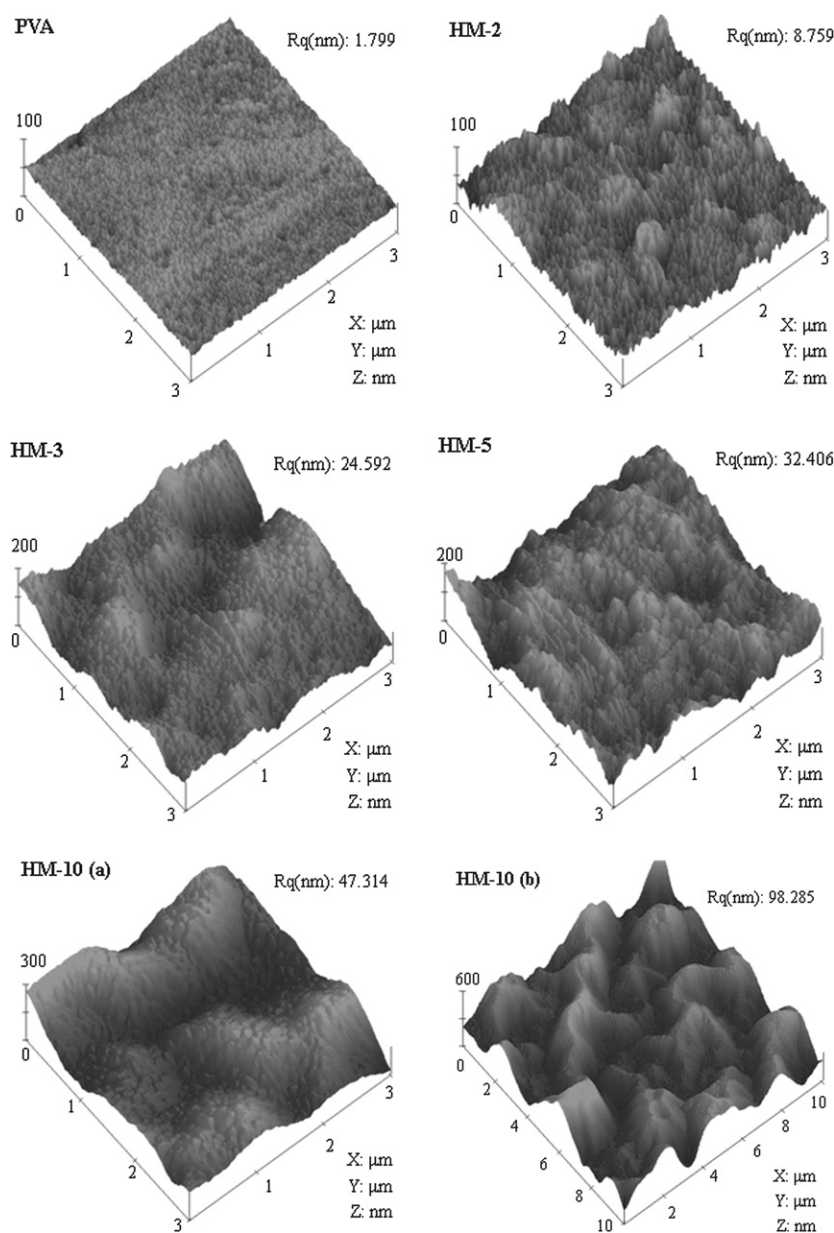


Fig. 6 3D AFM topographic images of the surface of the PVA and hybrid membranes.

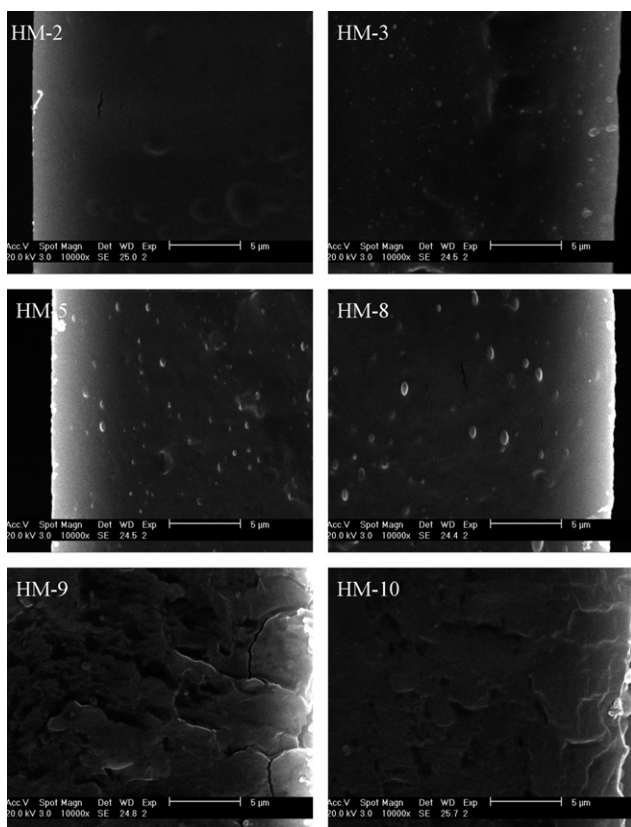


Fig. 7 SEM micrographs of the cross-section of the hybrid membranes.

In order to elucidate thoroughly the microstructure of the hybrid membranes, the bulk morphology of the HM-5 was characterized by TEM. Fig. 8 shows the TEM microphotograph of the HM-5. Silica particles appear and disperse uniformly in the hybrid membrane, and these particles are also observed by SEM. This is due to the PSS conglomeration in preparing the hybrid membranes, resulting in the formation of the PVA–silica nanocomposite membranes. The schematic structure of the HM-5 is displayed in Fig. 9. The PSS particles disperse homogeneously in

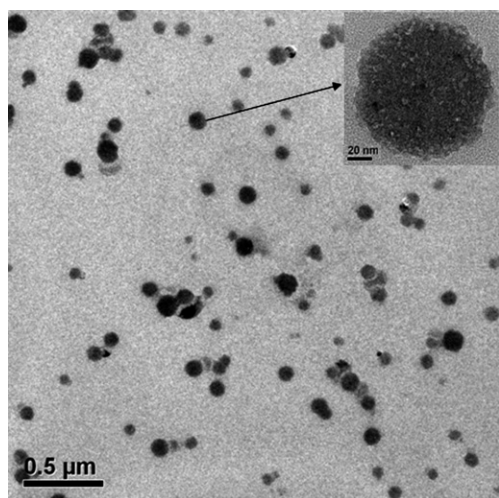


Fig. 8 TEM micrograph of HM-5.

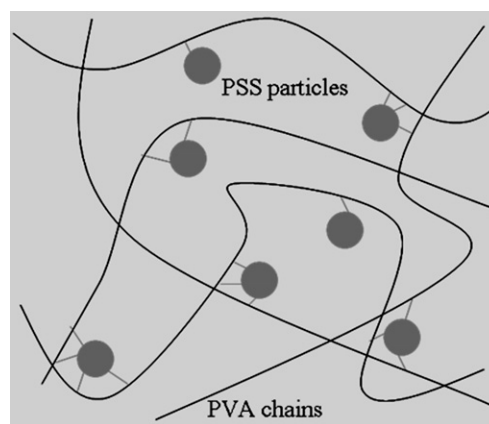


Fig. 9 Schematic structure of HM-5.

the PVA matrix and they link with the PVA chains by siloxane bonds.

Pervaporation performance of hybrid membranes

Fig. 10 shows pervaporation performances of the PVA and hybrid membranes in separation of a 90 wt% THF aqueous solution at 50 °C. It is found that the permeability and selectivity of the hybrid membranes is greater than the PVA membrane. The trade-off can be solved using the hybrid membranes. When the PSS content is below 2 wt%, the selectivity of the hybrid membranes increased sharply. This is due to an increase of the hydrophilicity of the hybrid membranes and the amorphous region of PVA becoming more compact. Furthermore, no silica particles can be observed and the PSS disperses homogeneously in the PVA matrix. Therefore the pore size in the membrane is small and large molecules such as THF may not penetrate through the membrane, resulting in an increase in water permselectivity. When the PSS content increases above 2%, the hydrophilicity of the hybrid membranes decreases, silica particles form and pore size increases. Larger pores allow THF to diffuse freely through the membrane and decrease water permselectivity. On the other hand, flux increases rapidly due to an increase in the free volume of the hybrid membranes with increasing PSS content, which is confirmed by XRD spectra and SEM.

Diffusion coefficient is an important factor to assess the penetrants diffusion through membranes. Based on Fick's law of diffusion, the diffusion coefficient in pervaporation can be calculated from the equation²⁶

$$D_i = \frac{J_i \delta}{C_i} \quad (3)$$

where J_i , D_i and C_i are the permeation flux ($\text{kg m}^{-2} \text{s}^{-1}$), diffusion coefficient ($\text{m}^2 \text{s}^{-1}$) and concentration of component i in the feed side of membranes (kg m^{-3}). δ is the diffusion length (m).

Fig. 11 shows the diffusion coefficients of water (D_{water}) and THF (D_{THF}) through the hybrid membranes at 50 °C. It is found that D_{water} is much greater than D_{THF} . This indicates that the PVA and hybrid membranes have good water permselectivity. With increasing PSS content, D_{water} increased progressively, while D_{THF} decreased at first and then increased linearly when the PSS content was above 2 wt%. This is because incorporating PSS

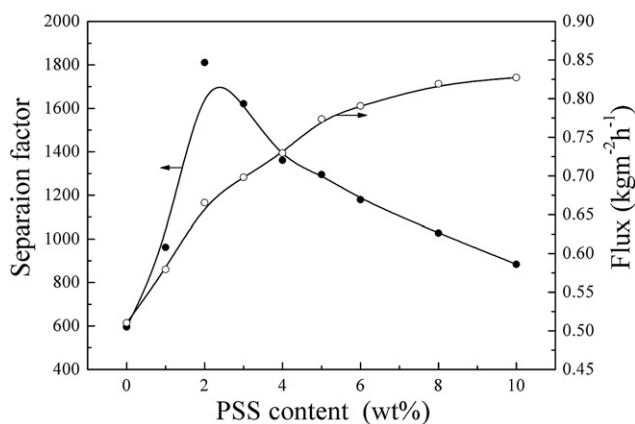


Fig. 10 Pervaporation performances of the hybrid membranes in the separation of 90 wt% THF solution at 50 °C.

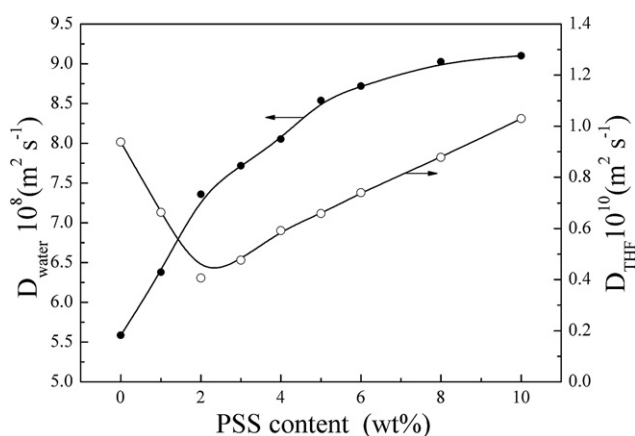


Fig. 11 Diffusion coefficients of water and THF permeating through the hybrid membranes at 50 °C.

into the PVA matrix leads to a decrease in the crystalline region of PVA which favors penetrant diffusion and results in an increase in D_{water} . However, the amorphous regions of PVA become more compact, which prevents the diffusion of larger molecules due to a size-exclusion action, resulting in a decrease in D_{THF} . Silica particles form and pores form around the silica particles when the PSS content is above 2%. These pores allow THF to diffuse freely, resulting in an increase in THF flux.

Conclusions

Novel organic-inorganic hybrid membranes containing poly(vinyl alcohol) (PVA) and polysilsesquioxane (PSS) were prepared successfully for the pervaporation dehydration of tetrahydrofuran. PSS (with molecular weight about 1000–2000 $\text{g}\cdot\text{mol}^{-1}$) was synthesized from (γ -aminopropyl)triethoxysilane by a sol-gel reaction, and the physico-chemical structures of the hybrid membranes were investigated by NMR, FTIR, AFM, TEM, etc. The PVA links with the PSS through siloxane bond in the hybrid membranes, and the incorporation of the PSS results in a decrease of the PVA crystalline region. The PSS congregates and silica particles form when the PSS content is above 2 wt%, and silica particles grew bigger with increasing PSS content. The

roughness of the hybrid membranes surface (R_q) increased linearly. Ridges and valleys were observed on the surface of the hybrid membranes, which became bigger with increasing PSS content.

The trade-off between the permeability and selectivity of PVA was successfully solved by the incorporation of the PSS into the PVA matrix. The flux through the hybrid membranes increased with increasing PSS content, whereas the water permselectivity of the hybrid membranes increased sharply with increasing PSS content up to 2 wt%, and then decreased. The hybrid membrane containing 2 wt% PSS exhibits the highest separation factor of 1810.

Acknowledgements

The support of National Nature Science Foundation of China (no. 50573063), the Program for New Century Excellent Talents in University and the research fund for the Doctoral Program of Higher Education (no. 2005038401) in the preparation of this article is gratefully acknowledged. The authors are grateful to B. W. Mao and J. W. Yan (State Key Laboratory for Physical Chemistry of Solid Surfaces and Department of Chemistry, College of Chemistry and Chemical Engineering, Xiamen University) for the assistance in AFM measurement and analysis.

References

- S. I. Semenova, H. Ohya and K. Soontarapa, *Desalination*, 1997, **110**, 251.
- A. Urtiaga, E. D. Gorri, C. Casado and I. Ortiz, *Sep. Purif. Tech.*, 2003, **32**, 207.
- B. D. Freeman, *Macromolecules*, 1999, **32**, 375.
- L. M. Robeson, *Curr. Opin. Solid State Mater. Sci.*, 1999, **4**, 549.
- S. J. Lue and S. H. Peng, *J. Membr. Sci.*, 2003, **222**, 203.
- P. Bahukudumbi and D. M. Ford, *Ind. Eng. Chem. Res.*, 2006, **45**, 5640.
- K. J. Shea and D. A. Loy, *Chem. Mater.*, 2001, **13**, 3306.
- L. Cot, A. Ayril, J. Durand, C. Guizard, N. Hovnanian, A. Julbe and A. Larbot, *Solid State Sci.*, 2000, **2**, 313.
- C. Sanchez, B. Julián, P. Belleville and M. Popall, *J. Mater. Chem.*, 2005, **15**, 3559.
- C. Guizard, A. Bac, M. Barboiu and N. Hovnanian, *Sep. Purif. Tech.*, 200, **25**, 167.
- B. Boury and R. J. P. Corriu, *Chem. Commun.*, 2002, 795.
- F. Pereira, K. Vallé, P. Belleville, A. Morin, S. Lambert and C. Sanchez, *Chem. Mater.*, 2008, **20**, 1710.
- B. Baradie, J. P. Dodelet and D. Guay, *J. Electroanal. Chem.*, 2000, **489**, 101.
- T. Tezuka, K. Tadanaga, A. Hayashi and M. Tatsumisago, *J. Am. Chem. Soc.*, 2006, **128**, 16470.
- C. Cornelius, C. Hibshman and E. Marand, *Sep. Purif. Tech.*, 2001, **25**, 181.
- G. V. R. Rao, M. E. Krug, S. Balamurugan, H. Xu, Q. Xu and G. P. López, *Chem. Mater.*, 2002, **14**, 5075.
- Y. L. Liu, Y. H. Su, K. R. Lee and J. Y. Lai, *J. Membr. Sci.*, 2005, **251**, 233.
- Y. L. Liu, Y. H. Su and J. Y. Lai, *Polymer*, 2004, **45**, 6831.
- T. Urugami, T. Katayama, T. Miyata, H. Tamura, T. Shiraiwa and A. Higuchi, *Biomacromolecules*, 2004, **5**, 1567.
- T. Ohshima, M. Matsumoto, T. Miyata and T. Urugami, *Macromol. Chem. Phys.*, 2005, **206**, 1638.
- K. Kusakabe, S. Yoneshige and S. Morooka, *J. Membr. Sci.*, 1998, **149**, 29.
- T. Urugami, H. Matsugi and T. Miyata, *Macromolecules*, 2005, **38**, 8440.
- T. Urugami, K. Okazaki, H. Matsugi and T. Miyata, *Macromolecules*, 2002, **35**, 9156.

- 24 F. Peng, L. Lu, H. Sun, Y. Wang, J. Liu and Z. Jiang, *Chem. Mater.*, 2005, **17**, 6790.
- 25 Q. G. Zhang, Q. L. Liu, Y. Chen and J. H. Chen, *Ind. Eng. Chem. Res.*, 2007, **46**, 913.
- 26 Q. G. Zhang, Q. L. Liu, Z. Y. Jiang and Y. Chen, *J. Membr. Sci.*, 2007, **287**, 237.
- 27 N. Algezewi, O. Sanli, L. Aras and G. Asman, *Chem. Eng. Process.*, 2005, **44**, 51.
- 28 C. K. Yeom and K. H. Lee, *J. Membr. Sci.*, 1996, **109**, 257.
- 29 A. A. Kittur, M. Y. Kariduraganavar, U. S. Toti, K. Ramesh and T. M. Aminabhavi, *J. Appl. Polym. Sci.*, 2003, **90**, 2441.
- 30 B. V. K. Naidu, M. Sairam, K. V. S. N. Raju and T. M. Aminabhavi, *J. Membr. Sci.*, 2005, **260**, 142.
- 31 M. Y. Kariduraganavar, S. S. Kulkarni and A. A. Kittur, *J. Membr. Sci.*, 2005, **246**, 83.
- 32 S. S. Kulkarni, A. A. Kittur, M. I. Aralaguppi and M. Y. Kariduraganavar, *J. Appl. Polym. Sci.*, 2004, **94**, 1304.
- 33 Q. G. Zhang, Q. L. Liu, J. Lin, J. H. Chen and A. M. Zhu, *J. Mater. Chem.*, 2007, **17**, 4889.
- 34 Q. G. Zhang, Q. L. Liu, Z. Y. Jiang, L. Y. Ye and X. H. Zhang, *Microporous Mesoporous Mater.*, 2008, **110**, 379.
- 35 H. Y. Chang, R. Thangamuthu and C. W. Lin, *J. Membr. Sci.*, 2004, **228**, 217.
- 36 M.-C. Brochier Salon, M. Abdelmouleh, S. Boufi, M. Naceur Belgacem and A. Gandini, *J. Colloid Interface Sci.*, 2005, **289**, 249.